

00/02/23

**MASS TRANSFER TO SPHERE AND
HEMISPHERE ELECTRODES BY AN
IMPINGING JET**

Eiran Kochavi, Yoram Oren, Abraham Tamir, Tuvia Kravchik

**BEN-GURION UNIVERSITY OF THE NEGEV, FACULTY OF
ENGINEERING SCIENCES, DEPARTMENT OF CHEMICAL
ENGINEERING. P.O.B 653, BEER-SHEVA, 84105, ISRAEL**

PHOENICS X11 – Version 2.1.3

Operating system – UNIX

ABSTRACT

Mass transfer rates from an impinging jet to sphere and hemisphere electrode are investigated using the electrochemical reduction of ferricyanid ion ($Fe[CN]_6^{-3}$) to ferrocyanide ($Fe[CN]_6^{-4}$). Measurements of mass transfer rates were made by using the limiting current technique. A theoretical model that characterizes the system of impinging jet to electrodes has been developed. Using a **numerical simulation program (PHOENICS)** the appropriate conservation equations are solved in the domain of solution.

The following experimental results were obtained:

1. Mass transfer coefficients for the hemisphere electrode are larger than those for the sphere electrodes, in both unsubmerged and submerged systems.
2. Mass transfer coefficients decrease by increasing the nozzle-electrode distance.
3. Mass transfer coefficients for the hemisphere electrode under submerged conditions are higher than those for an unsubmerged system. No significant differences between a submerged and an unsubmerged system were observed for the sphere electrode.

The results of the simulation are presented as velocity and concentration field distributions. Limiting current values, by comparison to experimental results, were in a good agreement.

<u>Content list</u>	<u>page</u>
1. Objective of work	4
2. The impinging jet electrode	5
3. The experimental system	6
4. Scheme of the experimental system	7
5. The theoretical model and PHOENICS settings	8
6. Scheme of solution domain	9
7. Result and discussion	10
8. Concentration profile	11
9. Flow vectors map	12
10. Convergence	13
11. Relaxation	13
12. Conclusions	14
13. Recommendations	14
14. Literature references	15
15. Appendix 1	15

1. Objective of work

The goals of this work were:

1. Characterization of mass transfer rates to sphere and hemisphere electrodes.
2. Characterization of mass transfer with both electrodes in two systems: the electrodes are submerged in the electrolyte solution and, in the second, the electrodes are unsubmerged.
3. Development of theoretical model that characterizes the system of impinging jet to electrodes.
4. Compare between the experimental limiting current values and the theoretical one.
5. Prediction of flow and concentration profiles at complex geometry system by using a **numerical simulation program (PHOENICS)** with the proper boundary conditions.

2. The impinging jet electrode

The impinging jet electrode is commonly used in electrochemical machining, Erosion corrosion, and other industrial processes. The flow characteristic of the impinging jet has been studied by a number of investigators (1-5). There was different geometry of the electrodes: Disk, Flat plate and Cylindrical plate.

Some investigators (6,7) made their research on heat and mass transfer from the impinging jet to the flat plate.

At the impinging jet electrode very high current densities can be achieved. In addition uniform mass transfer rates can be achieved, and this is the reason for using these electrodes, in selective electroplating processes.

3. The experimental system

The experimental system is presented at page no. 7.

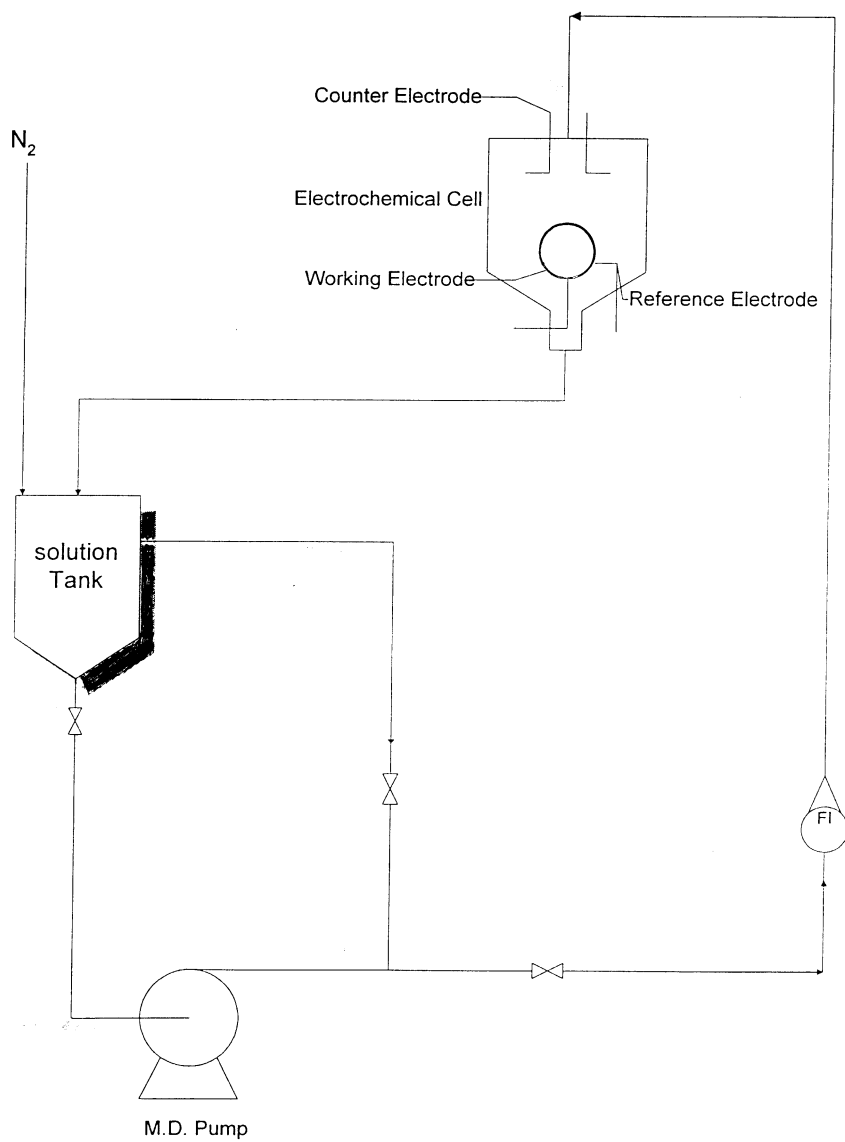
A jet of electrolyte impinged at the surface of a sphere electrode (working electrode). There are two different flow regimes: submerged and unsubmerged.

In a submerged flow the jet is flow through the solution that filled the electrochemical cell. The working electrode is submerged in the electrolyte.

In an unsubmerged flow the jet is surrounded by gas phase (Air). The working electrode is not submerged in the electrolyte

The electrolyte solution was made of: NaOH 2M, ferricyanid ion ($Fe[CN]_6^{-3}$) $5 \cdot 10^{-3}$ M and ferrocyanide ($Fe[CN]_6^{-4}$) $5 \cdot 10^{-2}$ M.

Determination of mass transfer rates was made using the limiting current technique. In this technique we measure the current vs. the supplied voltage Which cause the reduction reaction of ferricyanid ion ($Fe[CN]_6^{-3}$) to ferrocyanide ($Fe[CN]_6^{-4}$). The measurements were made at the Plateau region, where there is no significant change at the current, when we raise the supplied voltage.



4. Scheme of the experimental system

5. The theoretical model and PHOENICS settings

The impingement of electrolyte jet on a submerged sphere electrode, causes flow distribution perpendicular to surface of the electrode, and therefore concentration distribution at the same direction.

The model employed a 41x37 grid cells (BFC) in the y-z plane. The cells region has divided to 2 frames: in the first one the solution flew out of the nozzle and the method of the interpolation of internal points was transfinite (TRANS).

In the second frame the solution impinging the electrode and flew over it to the outlet. The method of the interpolation of internal points was “Laplace”-like equation (LAP). The grid distribution was also divided into 2 sections (in Y-axis). In the first one (20 cells) the distribution was **power-law** expanding grid to enable economical grid refinement and accuracy close to the surface. In the second one (20 cells) the distribution was **uniform** grid. The solution domain is shown schematically at page 9.

The model assumptions were:

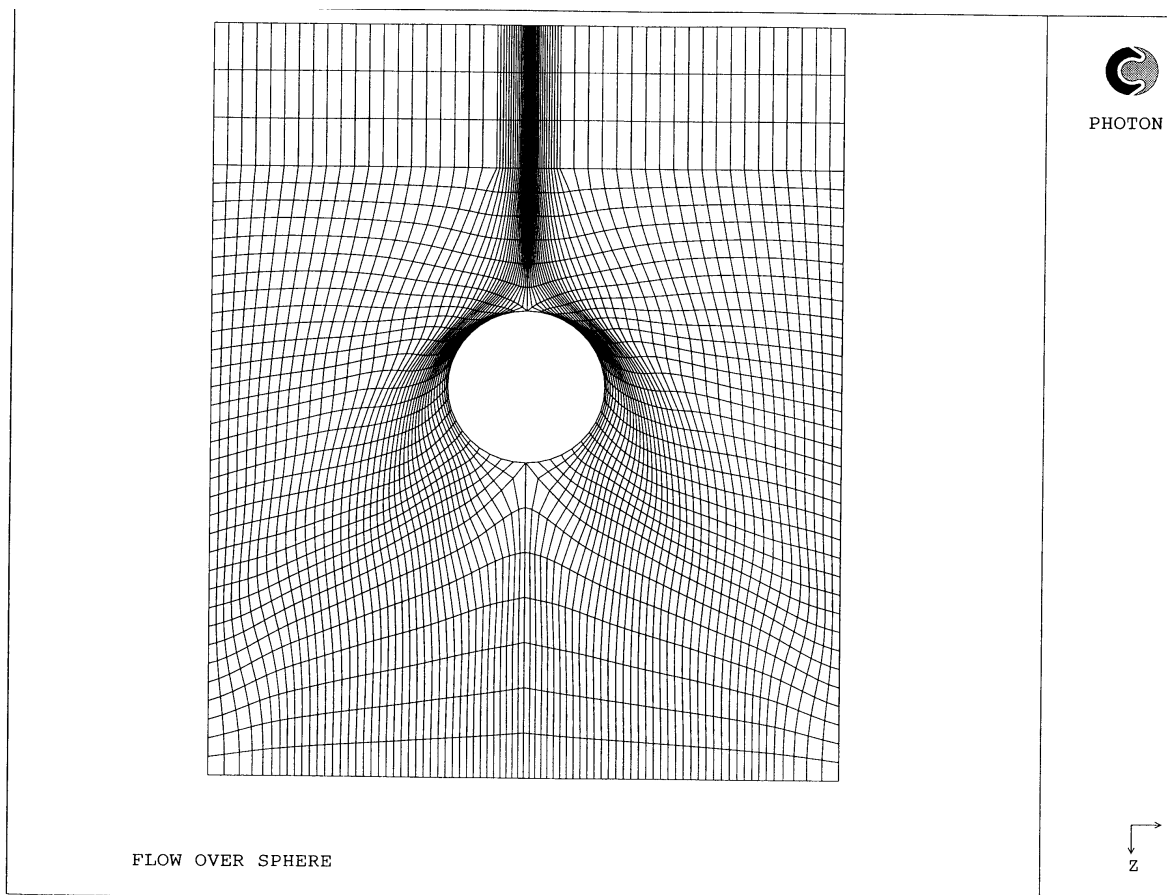
1. Steady-state condition
2. The electrochemical cell diameter is large enough, that we can neglect the walls influence on the flow boundary layer.
3. The physical properties of the electrolyte are identity in the nozzle, near the electrode and in the electrochemical cell
4. The influence of the gravity force is negligible

5. A full symmetry for Z-axis

6. Uniform temperature in the domain of solution.

The full code listing (Q1 file) for the numerical simulation of flow profile and mass transfer to submerged sphere electrode is presented at appendix 1.

6. Scheme of solution domain



7. Results and discussion

The following experimental results were obtained:

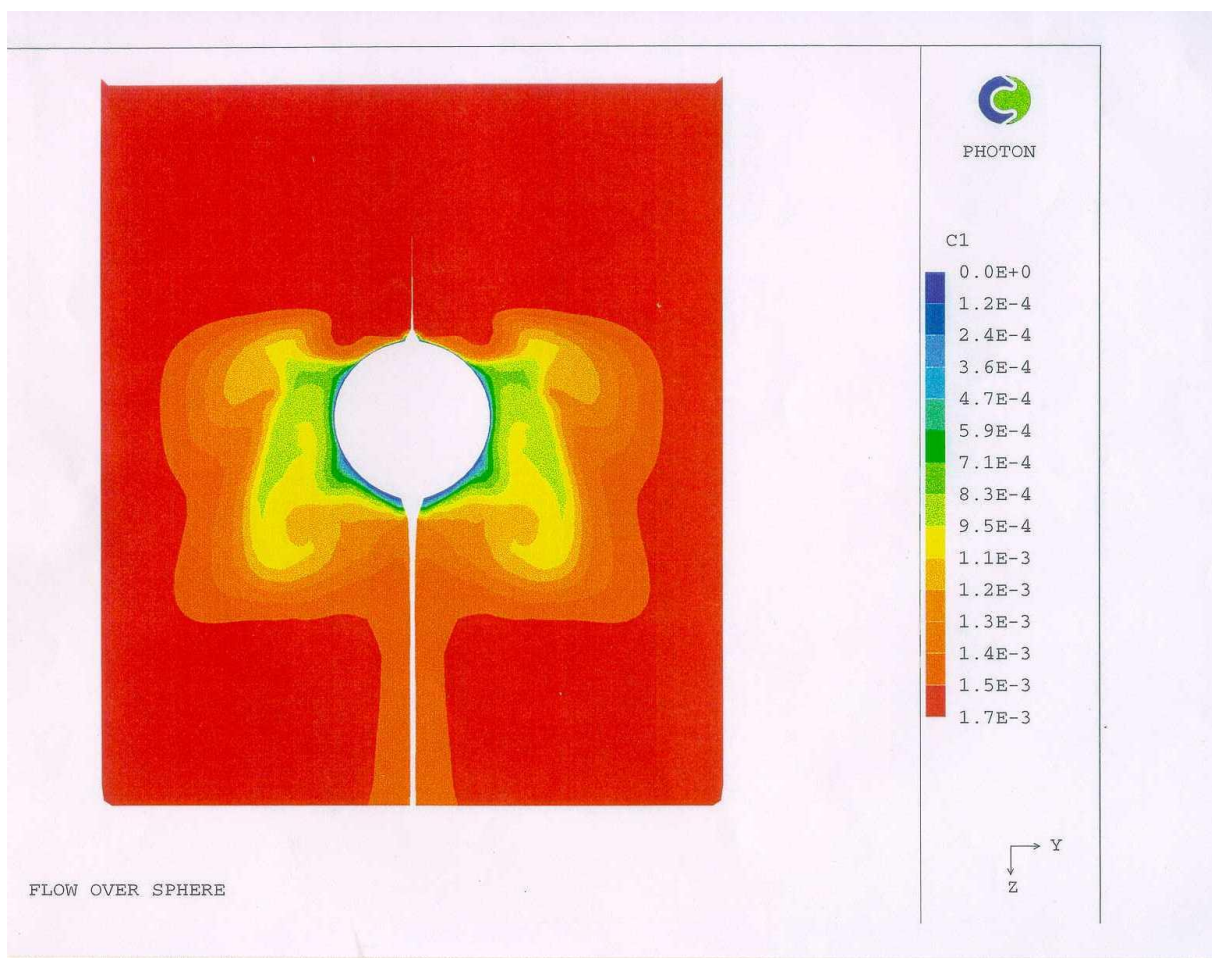
- Mass transfer coefficients for the hemisphere electrode are larger than those for the sphere electrodes, in unsubmerged and submerged electrodes.
- Mass transfer coefficients decrease by increasing the nozzle-electrode Distance (h). However, the influence is more pronounced at smaller distances (h = 1, 2, 8 mm) than the larger one (h = 14, 28 mm).
- Mass transfer coefficients for the hemisphere electrode under submerged conditions, are higher than the coefficients for an unsubmerged system. No significant differences between a submerged and an unsubmerged system were observed for the sphere electrode.

The theoretical results obtained for impinging jet on a submerged sphere electrode.

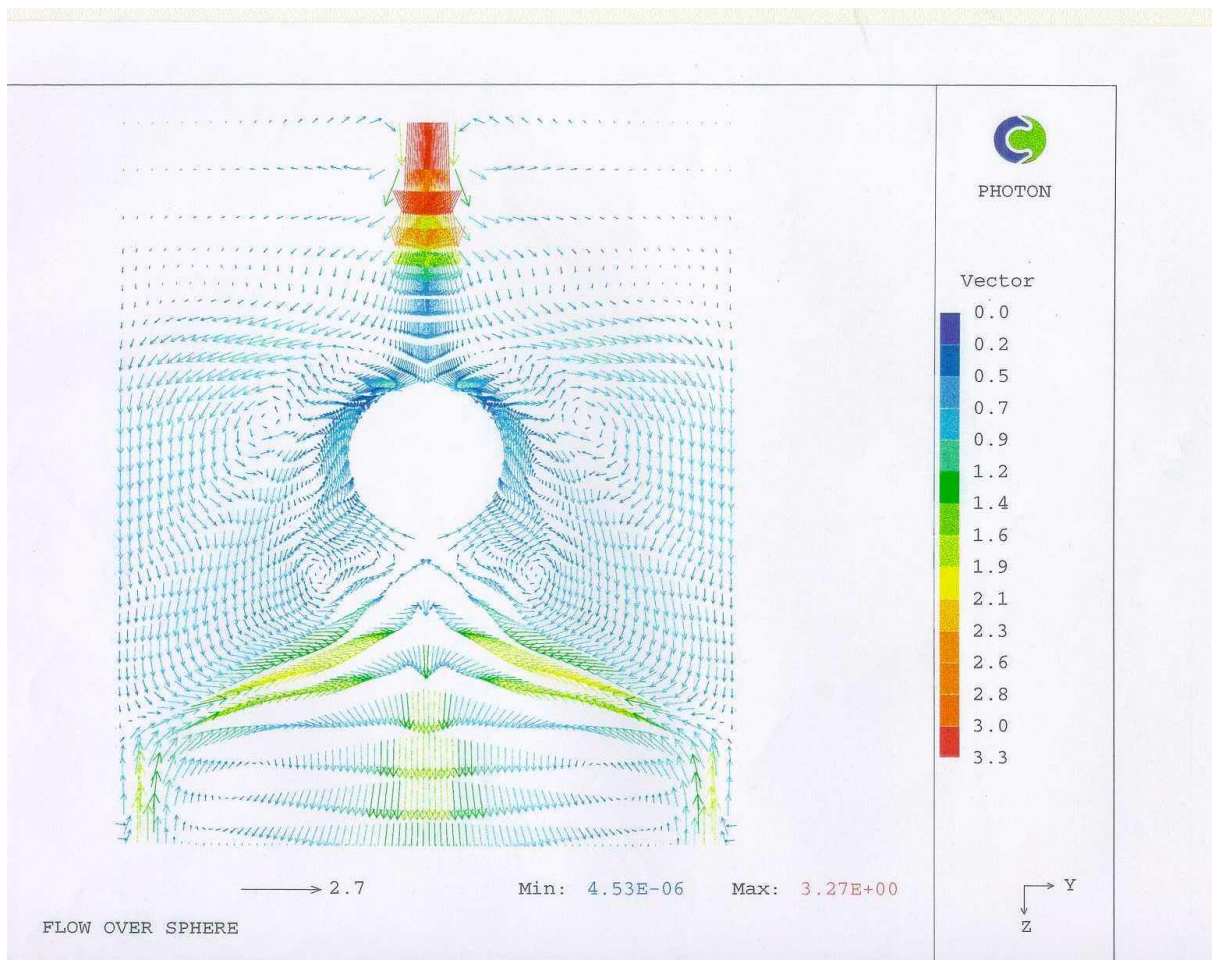
The theoretical current densities were calculated from the simulation results for ferricyanid ion mass fraction (concentration). These results are presented as distribution of ferricyanid ion mass fraction (page 11) and flow vectors map (page 12) for the domain of solution.

- At the impingement zone we observed a sharp concentration profile that influenced by jet impingement on the electrode surface.
- Because of the vortex (at the flow vectors map) on the electrode sides we observed the concentration profile to become wider along Z-axis.

8. Concentration profile of impinging jet over a submerged sphere electrode



9. Flow vectors map of impinging jet over a submerged sphere electrode



10. Convergence

The number of sweeps needed to get the theoretical results was 2000.

When we tried to raise the number of sweeps (2500, 3000) there were small changes in the values of the dependent variables.

11. Relaxation

The Relaxation factors for the variables were:

1. P1 – pressure, linear relaxation (LINRLX), 0.01
2. C1 – mass fraction of ferricyanid ion, linear relaxation (LINRLX), 0.01
3. C2 – mass fraction of water, linear relaxation (LINRLX), 0.01
4. V1 – velocity vector in Y-axis, false-time-step relaxation (FALSDT), $1 \cdot 10^{-5}$
5. W1 – velocity vector in Z-axis, false-time-step relaxation (FALSDT), $1 \cdot 10^{-6}$

The average time for the computer to get the theoretical results was 3 minuets.

12. CONCLUSIONS

1. Mass transfer coefficients for the hemisphere electrode are larger than those for the sphere electrodes, in unsubmerged and submerged electrodes. The reason for this is explained by the relatively small contribution, for mass transfer rate by lower part of the sphere electrode. The thickness of the diffusion boundary layer at that part, is bigger than the upper part at the impinging zone.

2. Calculated limiting currents from the concentration field distribution, were in a good agreement (0.5-10 %) by comparison to experimental results.

Using a numerical simulation code (PHOENICS) enables us to develop a method to predict the theoretical limiting current values.

13. RECOMMENDATIONS

1. Development of theoretical model for submerged hemisphere electrode and compare the results with the experimental one (it is done in these days actually).

2. Developments of theoretical model for unsubmerged sphere and hemisphere electrode, and compare the results with the experimental one.

3. Examination the possibilities of using sphere and hemisphere electrode, for electrochemical uses.

14. Literature references

- [1] D.T. Chin and C.H. Tsang, *J. Electrochem. Soc.* 125 (1978) 1461
- [2] K-L. Hsueh and D.T. Chin, *J. Electrochem. Soc.* 133 (1986) 75
- [3] K-L. Hsueh and D.T. Chin, *J. Electrochem. Soc.* 133 (1986) 1845
- [4] D.T. Chin and K.L. Hsueh, *J. Electrochim. Acta.* 31 (1986) 561
- [5] J. Nanzer, A. Doingeau, F. Coeuret, *J. of App. Electro.*, 14 (1986) 51
- [6] V.E. Nakoryakov, B.G. Pokusaev and E.N. Troyan, *J. Heat Mass Transfer*, 21 (1978) 1175.
- [7] P.A.M.S.G. Mohamed and G.J. Jameson, *Chem. Eng. Sci.*, 48 (1993) 489

15. Appendix 1

Code listing (Q1 file) for the numerical simulation of flow profile and mass transfer to submerged sphere electrode.

```

TALK=T;RUN( 1, 1);VDU=X11-TERM
IRUNN   =      1 ;LIBREF =      0
*****
Group 1. Run Title

TEXT(FLOW OVER SPHERE
*****
Group 2. Transience

STEADY =      T
*****
Groups 3, 4, 5 Grid Information
* Overall number of cells, RSET(M,NX,NY,NZ,tolerance)
RSET(M,1,41,37)
* Overall domain extent, RSET(D,name,XULAST,YVLAST,ZWLAST)
RSET(D,CHAM,0.03,0.03,0.074)
*****
Group 6. Body-Fitted coordinates

BFC=T
* Set points
GSET(P,P2,0.0000E+00,0.03,0.0000E+00)
GSET(P,P7,0.0000E+00,0.03,0.074)
GSET(P,P8,0.0000E+00,0.0000E+00,0.074)
GSET(P,P9,0.0000E+00,0.0000E+00,0.043)
GSET(P,P11,0.0000E+00,0.0000E+00,0.028)
GSET(P,P1,0.0000E+00,0.0000E+00,0.0000E+00)
GSET(P,P10,0.0000E+00,0.0075,0.0355)
GSET(P,P3,0.0,0.003,0.0)
GSET(P,P20,0.0,0.03,0.014)
GSET(P,P21,0.0,0.003,0.014)
GSET(P,P22,0.0,0.00,0.014)

* Set lines/arcs
GSET(L,L1,P3,P2,20,1.0)
GSET(L,L2,P20,P7,33,1.0)
GSET(L,L3,P1,P3,20, 2.43)
GSET(L,L10,P20,P21,20,1.0)
GSET(L,L4,P7,P8,40,1.0)
GSET(L,L5,P8,P9,7,1.0)
GSET(L,L6,P11,P22,6,1.0)
GSET(L,L11,P22,P21,20,2.43)
GSET(L,L12,P2,P20,3,1.0)
GSET(L,L13,P1,P22,3,1.0)
GSET(L,A6,P9,P11,20,1.0,ARC,P10)
* Set frames
GSET(F,F1,P22,P21,P20,-,P7,-,P8,P9.P11)
GSET(F,F2,P1,P3,P2,-,P20,P21,P22,-)

* Match a grid mesh
GSET(M,F1,+J+K,1,1,4,LAP20.FFFFFT)
GSET(M,F2,+J+K,1,1,1,TRANS)
* Copy/Transfer/Block grid planes
GSET(C,I2,F,I1,+,0.03,0,0)
*****
NONORT =      T
* X-cyclic boundaries switched
*****
Group 7. Variables: STOREd,SOLVEd,NAMED

ONEPHS =      T
* Non-default variable names
NAME(43) =HPOR ; NAME(44) =NPOR
NAME(45) =EPOR ; NAME(46) =VPOR
NAME(47) =UCRT ; NAME(48) =WCRT
NAME(49) =RHO1 ; NAME(50) =VCRT
* Solved variables list
SOLVE(P1 ,V1 ,W1,C1,C2)
* Stored variables list
STORE(VCRT,RHO1,WCRT,UCRT,VPOR,EPOR,NPOR,HPOR)
SOLUTN(P1 ,Y,Y,Y,N,N,N)
PRNDTL(C1) = 1070
PRNDTL(C2)=9.4E-03
*****

```



```

Group 8. Terms & Devices
*****
Group 9. Properties

RHO1    = 1.042E+03
ENUL    = 0.94E-6
*****
Group 10. Inter-Phase Transfer Processes
*****
Group 11. Initialise Var/Porosity Fields

FIINIT(W1 ) = 4.5
FIINIT(C1) =1.66E-03
FIINIT(C2)=0.9983
CONPOR(BALL,0.0,SOUTH,1,1,1,1,10,29)

RSTGRD  =    F

INIADD  =    F
*****
Group 12. Convection and diffusion adjustments
*****
Group 13. Boundary & Special Sources

REAL(WIN);WIN=4.5

INLET (IN,LOW,1,NX,1,20,1,1,1,1)
VALUE (IN,P1 ,WIN*RHO1)
VALUE (IN,V1 ,0.0)
VALUE (IN,W1 ,WIN)

PATCH(IN1,CELL,1,NX,1,20,1,1,1,1)
COVAL(IN1,C1,FIXVAL,1.66E-03)
COVAL(IN1,C2,FIXVAL,0.9983)

WALL(WALIN,LOW,1,NX,21,NY,1,1,1,1)

OUTLET(OUT1,HIGH, 1, NX, 1, NY, NZ, NZ,1,1)
VALUE (OUT1,P1,0.0)
VALUE(OUT1,C1,1.66e-03)
VALUE(OUT1,C2,0.9983)

WALL(WBALL,SOUTH,1,NX,1,1,10,29,1,1)
WALL(OUTW,NORTH,1,NX,NY,NY,1,NZ,1,1)

PATCH(WBALL,SOUTH,1,NX,1,1,10,29,1,1)
COVAL(WBALL,C1,FIXVAL,0.0)
COVAL(WBALL,C2,FIXVAL,1.0)
*****
Group 14. Downstream Pressure For PARAB
IPARAB = 0
*****
Group 15. Terminate Sweeps

LSWEEP = 2000
SELREF = T
RESFAC = 1.000E-02
*****
group 16. Terminate Iterations
*****
Group 17. Relaxation

RELAX(P1 ,LINRLX, 0.01)
RELAX(V1,FALSDT,0.00001)
RELAX(W1,FALSDT,0.00001)
RELAX(C1,LINRLX,0.1)
RELAX(C2,LINRLX,0.1)
*****
Group 18. Limits

VARMIN(C1)=0.0; VARMAX(C1)=1.0

```

VARMIN(C2)=0.0; VARMAX(C2)=1.0

Group 19. EARTH Calls To GROUND Station

GENK = T

Group 20. Preliminary Printout

ECHO = T

Group 21. Print-out of Variables

OUTPUT(HPOR,N,N,N,Y,N,N)
OUTPUT(NPOR,N,N,N,Y,N,N)
OUTPUT(EPOR,N,N,N,Y,N,N)
OUTPUT(VPOR,N,N,N,Y,N,N)
OUTPUT(WCRT,N,N,N,N,N,N)
OUTPUT(VCRT,N,N,N,N,N,N)
OUTPUT(UCRT,N,N,N,N,N,N)
OUTPUT(RH01,N,N,N,N,N,N)

Group 22. Monitor Print-Out

IXMON=1
IYMON=1
IZMON=2
TSTSWP=-1

Group 23. Field Print-Out & Plot Control

ISWPRF=1000
ISWPRL=2000
NYPRIN=1
NZPRIN=1

Group 24. Dumps For Restarts

STOP